8. H. Hirai and K. Kondo, *Proc. Jpn. Acad.* **67(B)**, 22 (1991).
9. P. P. K. Smith and P. R. Buseck, *Science* **216**, 984 (1982).
10. D. E. Grady, *J. Geophys. Res.* **85**, 913 (1980).
11. K. Kondo, A. Sawaoka, S. Saito, in *High-Pressure Science and Technology*, K. D. Timmerhaus and M. S. Barber, Eds. (Plenum, New York, 1971), vol. 2, pp. 905–910.
12. Static experiments on graphite compression at room temperature made by M. Hanfland *et al.* [*Phys. Rev. B* **39**, 12598 (1989)], Y. X. Zhao and J. L. Spain [*ibid.* **40**, 993 (1989)], and A. F. Goncharov *et al.* [*Sov. Phys. JETP* **69**, 380 (1989)] showed a few phases suggesting "proto" hexagonal diamond. Comparing the reported *d* spacings with those of n-diamond, n-diamond is different from any of these phases (*8*).
13. H. Vora and T. J. Moravec, *J. Appl. Phys.* **52**, 6151 (1981).
14. We thank M. Kitamura for valuable discussions and S. Sawai and K. Sakuta for help in developing the technique.

21 March 1991; accepted 5 June 1991

Observations of Extreme Upwelling Filaments in the Southeast Atlantic Ocean

J. R. E. LUTJEHARMS, F. A. SHILLINGTON, C. M. DUNCOMBE RAE

Cold oceanic water upwells along the western coastline of most major continents. The thermal front that demarcates the farthest seaward extent of this upwelled water is sometimes characterized by extensive whisps or cross-frontal filaments. These may play an important role in the functioning of the upwelling ecosystem as a whole. Satellite observations on filaments of the Benguela upwelling system show filaments that exceed 1000 kilometers in length. Two mechanisms that may produce the exceptional length of these filaments are interaction with Agulhas rings and the effect of intense berg winds.

OCEANIC UPWELLING REGIMES PLAY a principal role in the ecology of the eastern boundary areas of most ocean basins, in particular that of the Northeast Pacific (*1*), Southeast Pacific (*2*), and Southeast Atlantic oceans (*3*). It has been suggested that in many instances biological productivity of upwelling areas is concentrated at the fronts that separate cold upwelled water from the adjacent ocean surface water (*4*). Frontal behaviour may therefore be an important element in the potential primary productivity of upwelling areas as a whole. Moreover, by raising deeper water to the sea surface where it is warmed by insolation and atmosphere-to-ocean heat transfer, upwelling regimes modify the temperature and salinity of substantial volumes of water. The full areal extent of upwelling regimes, as delimited by their upwelling fronts, is therefore a factor in global water mass modification and thus by implication in climate. With the advent of satellite remote sensing it has become increasingly evident that upwelling fronts are, usually, not smooth but consist of a heterogeneous collection of mesoscale plumes, whisps, and filaments (*5*); these features significantly extend both the productive habitat associated with the front (*6*) as well as the areal extent of cold surface water. The full geographic extent of these filaments in each individual upwelling regime has yet to be established. In this report, we describe unusually elongated filaments of the Benguela upwelling system in the Southeast Atlantic.

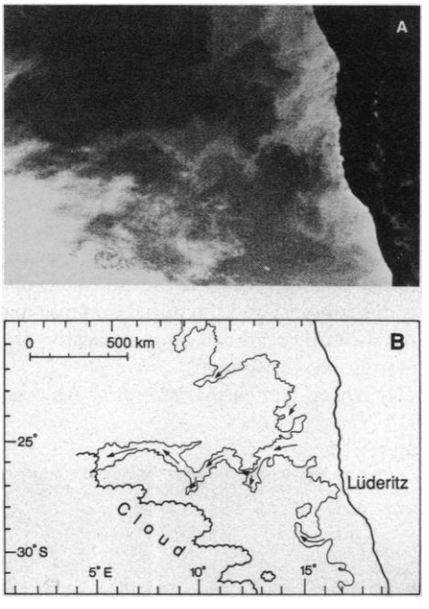

Fig. 1. (**A**) Thermal infrared image of the upwelling area of the Southeast Atlantic Ocean from the METEOSAT II satellite for 5 July 1982. Colder water is indicated by lighter hues. An extreme, meandering upwelling filament is evident off Lüderitz. (**B**) Interpretive sketch of the same scene with lines of latitude and longitude. An approximate kilometer scale is given as reference.

The upwelling regime of the Southeast Atlantic Ocean stretches from the Benguela-Angolan front at about 16°S to Cape Agulhas (*3*), the most southern tip of Africa. Upwelling occurs preferentially in certain specific upwelling cells (*7*), the location of which in many cases corresponds to narrow parts of the continental shelf (*3*). The central and most intense of these upwelling cells is the one at Lüderitz (27°S) (*8*). On average its surface water is colder than that in other upwelling cells, it extends farther offshore, and it exhibits active upwelling more frequently than any of the other identified cells (*7*). Upwelling filaments typically form on the fronts of all cells where the upwelling is well developed (*9*). This filamentous band, parallel to and seaward of the main, contiguous upwelled water, is usually between 100 and 500 km wide (*10*).

Upwelling filaments of this kind have been shown to have certain distinctive characteristics. They are quasi-geostrophic jets that entrain cold water at coastal upwelling sites and rapidly advect it far offshore (*11*). This flow pattern probably provides significant cross-shore transport of heat, nutrients, biota, as well as pollutants, and may be associated with adjacent mesoscale eddies (*12*). Measurement of the kinematic characteristics of such filament features in the California Current system (*13*) have shown that under certain conditions the flow configuration consists of a rapid offshore flow balanced by a slower, parallel return flow that converges at the front on the equatorward side of the filament. Filaments may extend to a depth of 100 m (*14*), last a number of weeks, and may carry a volume flux in excess of 10^6 m^3/s (*13*).

The unusually long filaments were revealed in a study of a large collection of satellite thermal infrared images for the Southeast Atlantic Ocean covering more than 10 years (*15*) (Fig. 1). The filaments occasionally developed off the Lüderitz upwelling cell. Whereas most observed filaments extended about 300 km offshore (*13*), these extreme filaments off Lüderitz exceeded 1000 km in length.

An example of such an extreme upwelling filament is shown in Fig. 1. The filament had its origin in the surface upwelling front seaward of the continental shelf edge and extended more than 1300 km offshore. Sideways meanders with a wavelength of about 250 km and a wave amplitude of 100 km shaped the trajectory of the cold water (*16*). The surface expression of this extreme filament was persistent for about 10 days, from 5 to 14 July 1982. For this whole period it extended more than 1000 km offshore.

J. R. E. Lutjeharms and F. A. Shillington, Department of Oceanography, University of Cape Town, 7700 Rondebosch, South Africa.
C. M. Duncombe Rae, Department of Oceanography, University of Cape Town, 7700 Rondebosch and Sea Fisheries Research Institute, Private Bag X2, 8012 Roggebaai, South Africa.

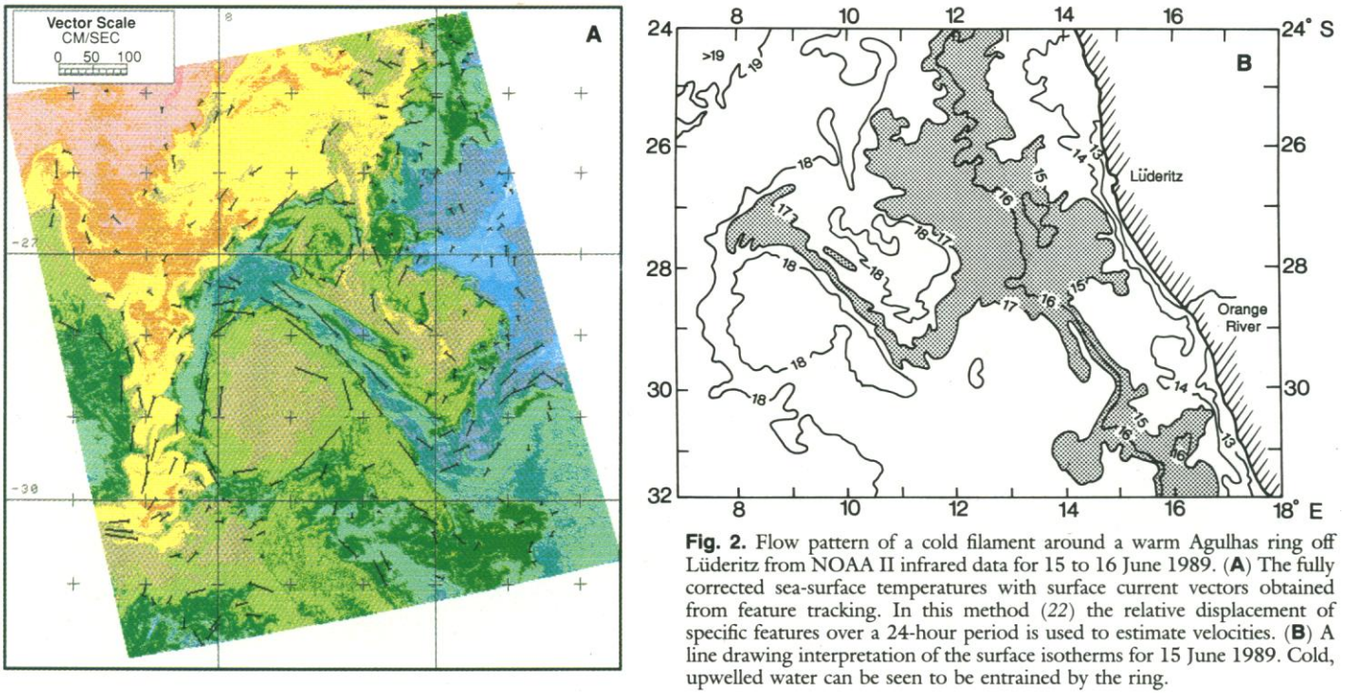

Fig. 2. Flow pattern of a cold filament around a warm Agulhas ring off Lüderitz from NOAA II infrared data for 15 to 16 June 1989. (**A**) The fully corrected sea-surface temperatures with surface current vectors obtained from feature tracking. In this method (*22*) the relative displacement of specific features over a 24-hour period is used to estimate velocities. (**B**) A line drawing interpretation of the surface isotherms for 15 June 1989. Cold, upwelled water can be seen to be entrained by the ring.

A mechanism responsible for carrying upwelling filaments so far offshore is suggested by the meandering shape of the filaments observed. This part of the ocean periodically contains a collection of Agulhas rings (*12, 17*) spawned at the Agulhas Current retroflection (*18*) farther south in the Southeast Atlantic Ocean. These rings generally drift in a northward and northwestward direction (*17, 19*). Interaction with upwelling filaments may lead to the partial entrainment of filaments along the periphery of one or more of such rings.

Our recent investigations at sea have confirmed this type of interaction. A research cruise to investigate an Agulhas ring in the South Atlantic Ocean was carried out in May 1989 (*12*). Satellite thermal infrared imagery for a period during and after the cruise revealed the envelopment of the ring by an extreme upwelling filament just south of Lüderitz (Fig. 2). The Agulhas ring was evident as an anticyclonic (anticlockwise), warm core (water at the center was 5°C warmer than ambient) feature in the hydrographic measurements down to a depth of at least 1200 m. Surface geostrophic velocities (*20*) were ~50 cm/s and were confirmed by the ship's drift during the survey.

Two hydrographic transects (a total of 20 stations) were conducted across the ring. Salinities in the upper 75 m at the northwest edge of the ring were anomalously low (35.3×10^{-3}); a value typically found at the upwelling frontal region (*3*) and also found recently in an upwelling filament near Lüderitz (*21*). These measurements confirm that the cool water being entrained by the ring, as shown in Fig. 2, is of upwelling origin. Surface currents in the filament (Fig. 2) varied between 40 cm/s near its upwelling origin and 60 cm/s near the eastern side of the ring. The filament stretched 770 km away from the coast, before its final southward entrapment around the ring. Using a conservative surface current speed of 30 cm/s, an average width of 50 km, and a depth of 100 m, we estimate that the offshore volume flux of the filament was 1.5×10^6 m^3/s.

The driving force for upwelling along southern Africa's west coast is a southeasterly wind associated with the anticyclonic air circulation around the South Atlantic high-pressure system. On occasion this system causes berg winds, a seaward flow of air that is adiabatically warmed as it moves from the high continental plateau down to sea level. Intense berg winds have on occasion been observed to carry sand and dust from the Namib desert up to 700 km offshore (*23*). Study of the best available satellite imagery for this ocean area, covering the period 1978 to 1984, indicated that at least 11 events occurred during which upwelling filaments off Lüderitz extended more than 500 km offshore. Each of these instances was apparently associated with particularly intense berg winds, which were indicated by the presence of extensive dust streaks in the satellite images. An analysis of the rate of seaward penetration of such long filaments shows that their reaction time to the onset of strong berg winds is within days.

These results demonstrate that the surface effects of the upwelling system of the Southeast Atlantic Ocean are on occasion observable much farther seaward than was conventionally thought to be the case. Long filaments are caused by the juxtaposition in this area of an extensive coastal upwelling system and a field of intense rings shed from a nearby western boundary current. The process may be enhanced by occasional high velocity offshore flows of air. The penetration of upwelled water into the central ocean basin has implications for the ecology of the surface water of the region as well as for the interpretation of deep-sea sediments of the area. Under intense offshore winds and increased ring shedding, such as predicted under some warmer climate scenarios (*24*), the surface extent of this upwelling system can be expanded and atmosphere-ocean heat transfer thus greatly augmented.

REFERENCES AND NOTES

1. K. H. Brink, D. W. Stewart, J. C. van Leer, *J. Phys. Oceanogr.* **14**, 378 (1984).
2. J. J. Walsh, J. C. Kelley, R. C. Dugdale, B. W. Frost, *Invest. Pesq.* **35**, 25 (1971).
3. L. V. Shannon, *Oceanogr. Mar. Biol. Annu. Rev.* **23**, 105 (1985).
4. B. H. Jones, L. P. Atkinson, D. Blasco, K. H. Brink, S. L. Smith, *Cont. Shelf Res.* **8**, 1155 (1988); D. A. Armstrong, B. A. Mitchell-Innes, F. Verheye-Dua, H. Waldron, L. Hutchings, *S. Afr. J. Mar. Sci.* **5**, 171 (1987).
5. K. H. Brink, *Progr. Oceanogr.* **12**, 223 (1983).
6. E. D. Traganza, J. C. Conrad, L. C. Breaker, in *Coastal Upwelling*, F. A. Richards, Ed. (American Geophysical Union, Washington, DC, 1981), pp.

228–241.
7. J. R. E. Lutjeharms and J. M. Meeuwis, *S. Afr. J. Mar. Sci.* **5**, 51 (1987).
8. R. H. Parrish, A. Bakun, D. M. Husby, C. S. Nelson, *F.A.O. Fish. Rep.* **291**, 731 (1983).
9. L. V. Shannon, N. M. Walters, S. A. Mostert, in *South African Ocean Colour and Upwelling Experiment*, L. V. Shannon, Ed. (Sea Fisheries Research Institute, Cape Town, 1985), pp. 183–210.
10. D. van Foreest, F. A. Shillington, R. Legeckis, *Cont. Shelf Res.* **3**, 465 (1984); J. R. E. Lutjeharms and P. L. Stockton, *S. Afr. J. Mar. Sci.* **5**, 35 (1987).
11. C. N. K. Mooers and A. R. Robinson, *Science* **223**, 51 (1984).
12. C. M. Duncombe Rae, L. V. Shannon, F. A. Shillington, *S. Afr. J. Sci.* **85**, 747 (1989).
13. P. Flament, L. Armi, L. Washburn, *J. Geophys. Res.* **90**, 11,765 (1985).
14. P. M. Kosro and A. Huyer, *ibid.* **91**, 7680 (1986).
15. Satellite imagery consisted of about 3700 daily images from the geostationary METEOSAT series measuring in the 10.5- to 12.5-μm range and having a subsatellite spatial resolution of 5 by 5 km, as well as about 1400 images from the NOAA, TIROS-N, and NIMBUS 7 polar orbiting satellite series. These three have a finer subsatellite resolution and measure in the 10.5- to 11.5-μm range. This collection covers the period 1978 to the present. Data received was not in all cases atmospherically or geometrically corrected, but was contrast-enhanced in the appropriate temperature range observed in this ocean area.
16. The termination of the filament by a southward bend (not shown here, but visible on 1 July 1982) coincided with the location of the Walvis Ridge, which shoals to a depth of about 2000 m below the sea surface at this point.
17. A. L. Gordon and W. F. Haxby, *J. Geophys. Res.* **95**, 3117 (1990).
18. J. R. E. Lutjeharms and A. L. Gordon, *Nature* **325**, 138 (1987); J. R. E. Lutjeharms and R. C. van Ballegooyen. *J. Phys. Oceanogr.* **18**, 1570 (1988).
19. D. B. Olson and R. H. Evans, *Deep-Sea Res.* **33**, 27 (1986).
20. Hydrographic measurements were carried out using a Neil Brown conductivity-temperature-depth (CTD) sensor. Geostrophic velocities based on this data were calculated relative to 1100 dB.
21. F. A. Shillington *et al.*, *Deep-Sea Res.* **37**, 1753 (1990).
22. J. J. Agenbag and L. V. Shannon, *S. Afr. J. Mar. Sci.* **6**, 119 (1988).
23. L. V. Shannon and F. P. Anderson, *S. Afr. J. Photogram. Rem. Sensing Cartogr.* **13**, 153 (1982).
24. A. Bakun, *Science* **247**, 198 (1990).
25. Satellite imagery was supplied by the Satellite Remote Sensing Centre of the Council for Scientific and Industrial Research at Hartebeesthoek and processed by J. Agenbag. A Fine-Resolution Antarctic Model (FRAM) Senior Visiting Fellowship from the National Environmental Research Council, UK, to J.R.E.L. made the completion of this investigation possible. The project was funded through the Benguela Ecology Programme of the Foundation for Research Development. We thank P. L. Stockton for help with the analyses and the captains and ship's crew of the Department of Environment Affairs' ships RV *Benguela* and RV *Africana* for help in obtaining hydrographic data.

8 January 1991; accepted 2 May 1991

Contact Adhesion of Thin Gold Films on Elastomeric Supports: Cold Welding Under Ambient Conditions

GREGORY S. FERGUSON, MANOJ K. CHAUDHURY, GEORGE B. SIGAL, GEORGE M. WHITESIDES*

Thin gold films placed in contact on compliant elastomeric poly(dimethylsiloxane) supports weld together. This "cold welding" is remarkable both for the low loads required and for the fact that it occurs under ambient laboratory conditions, conditions in which the gold surfaces are covered with films of weakly adsorbed organic impurities. These impurities are probably displaced laterally during the welding. Welding can be prevented by the presence of a self-assembled gold(I) alkylthiolate monolayer on the gold surfaces. The welded contacts have low electrical resistivity and can be made thin enough to transmit light. This system is a promising one with which to study interaction between interfaces.

WELDING OF METALS UNDER AMBIENT conditions ("cold welding") has been practiced for more than 700 years, but only with high applied pressures (such as under the impact of a smith's hammer) or with frictional work (*1–3*). The adhesion of metals in ultrahigh vacuum (UHV) under light loads is also known (*4*) but requires flat, ductile, and atomically clean surfaces. In this report we describe the self-adhesion of thin gold films on elastomeric supports, under ambient laboratory conditions, with very small applied loads (Fig. 1). Adhesive bonding of metal surfaces under ambient laboratory conditions—that is, in the presence of air, humidity, and volatile organic contaminants—and with very small applied loads (<0.1 to 0.2 g/cm^2) (*5*) is therefore remarkable. For self-adhesion of these "dirty," supported films of gold, an underlying elastomeric support is required. The self-adhesion is inhibited or prevented by monolayer films [self-assembled monolayers (SAMs)] less than 1 nm thick on the gold.

We prepared the systems by the procedure summarized in Fig. 1. Treatment of a film of poly(dimethylsiloxane) (PDMS) (*6*) with a radio frequency, oxygen plasma formed a thin [<50 Å by x-ray photoelectron spectroscopy (XPS)] silica-like layer on its surface. We denote this oxidized surface as PDMS/SiO_2: its surface chemistry is similar to that of SiO_2 (*7*). Chemisorption of 11-trichlorosilylundecyl thioacetate [$Cl_3Si(CH_2)_{11}SCOCH_3$] from the vapor phase onto PDMS/SiO_2 produced a monolayer of the corresponding alkylsiloxane (*8, 9*). Thin films of gold (~20 nm), thermally evaporated onto the surface of the PDMS-bound SAM (*9–11*), adhered well to it (*9, 12, 13*).

When placed in contact, two gold films supported on 1 cm by 1 cm squares of PDMS adhered strongly across the gold-gold interface. Failure occurred by decohesion within the polymer (the tear strength of the PDMS used here is 2.7×10^3 g/cm) (*14*). We hypothesize that the elasticity and compliance of PDMS allow the gold surfaces to conform to one another, increasing the area of gold-gold contact and tangentially displacing loosely adsorbed contaminants (*15*). This hypothesis implies the possible formation of "islands" of the contaminants at the gold-gold interface.

We measured the strength of adhesion by using an apparatus reported separately (*8*). A small (radius of curvature = 1.31 to 1.34 mm) hemispherical lens of PDMS and a flat sheet of PDMS were allowed to come into contact in the absence of an applied load. For two surfaces of unmodified PDMS, the pull-off force was 0.034 dyne for an initial area of contact at zero load of 4.45×10^{-4} cm^2. We characterize this adhesion as "tacky," because the area of contact decreased with increasing negative load. The pull-off force for the two gold films supported on PDMS was 3.33 dyne for an initial area of contact of 3.53×10^{-4} cm^2. In this case, the area of contact did not decrease with increasing negative load; rather, cohesive failure occurred within the flat sheet of PDMS. We conclude that this pull-off force is a lower limit of the strength of adhesion across the gold-gold interface and that these results rule out the possibility that the welding is actually tacky adhesion arising from organic contaminants at the interface.

Chemisorbed monolayers of alkyl thiolates at the surfaces of these gold films prevented welding. Treatment of one of the films with ethanoethiol vapor for 5 to 10 s greatly reduced the strength of adhesion; that is, the films were easily separated and adhesive failure occurred at the "gold-gold" interface. This "weak" adhesion was similar in strength and character to the tackiness between sheets of unmodified PDMS (*16*). As expected, gold films bearing ordered SAMs of longer chain alkyl thiolates (*17*)

G. S. Ferguson, G. B. Sigal, G. M. Whitesides, Department of Chemistry, Harvard University, Cambridge, MA 02138.
M. K. Chaudhury, Dow Corning Corporation, Midland, MI 48686.

*To whom correspondence should be addressed.